Early prediction of histopathological tumor response to preoperative chemotherapy by Tc-99m MIBI imaging in bone and soft tissue sarcomas

	Taki Junichi, Inaki Anri, Wakabayashi Hiroshi, Sumiya Hisashi, Tsuchiya Hiroyuki, Zen Yoh, Kinuya Seigo
journal or publication title	Clinical Nuclear Medicine
volume	35
number	3
page range	154-159
year	2010-03-01
URL	http://hdl.handle.net/2297/23484

Early Prediction of Histopathological Tumor Response to Preoperative Chemotherapy by Tc-99m MIBI imaging in Bone and Soft Tissue Sarcomas

Junichi Taki, MD, PhD[1], Anri Inaki, MD[2], Hiroshi Wakabayashi, MD[2], Hisashi Sumiya, MD, PhD[1], Hiroyuki Tsuchiya, MD, PhD[3], Yoh Zen, MD, PhD[4], Seigo Kinuya, MD, PhD[2]

[1]Department of Nuclear Medicine, Kanazawa University Hospital, [2]Department of Biotracer Medicine, Kanazawa University Graduate School of Medical Sciences, Kanazawa, Japan; [3]Department of Orthopedic Surgery, Kanazawa University Graduate School of Medical Sciences, Kanazawa, Japan; and [4]Division of Pathology, Kanazawa University Hospital, Kanazawa, Japan

Correspondence and reprint requests:

Junichi Taki

Department of Nuclear Medicine, Kanazawa University Hospital,

13-1 Takara-machi, Kanazawa, 920-8640, Japan

E-mail; taki@med.kanazawa-u.ac.jp

Tel; +81-76-265-2333, Fax;+81-76-234-4257,

Abstract.

Purpose: Tc-99m-MIBI accumulates in only viable cells. In patients with bone and soft tissue sarcomas, preoperative chemotherapy is essential and the early prediction of the tumor response to chemotherapy would be beneficial for the planning of treatment strategy. The purpose of this study was to assess whether the change of Tc-99m-MIBI image from pre-chemotherapy to the early to middle of the chemotherapy can predict final histopathological tumor response as accurately as the change of the image after completion of chemotherapy.

Methods: Seventy-three patients with bone and soft tissue sarcomas underwent Tc-99m-MIBI scintigraphy before chemotherapy and at least 2 times after the second or third or fifth chemotherapy. The change of the tracer uptake (ΔUR) and perfusion (ΔPI) from pre-chemotherapy to post-chemotherapy were compared with histologic response.

Results: The sensitivity, specificity, and accuracy for the prediction of effective chemotherapy in ΔPI were 88%, 83%, 85% after 2nd, 85%, 72%, 78% after 3rd, and 81%, 71%, 76% after 5th chemotherapy, and those in ΔUR were 88%, 83%, 85% after 2nd, 85%, 92%, 89% after 3rd, and 94%, 77%, 85% after 5th chemotherapy, respectively. The area under the receiver operator characteristic curve of the ΔPI after 2nd, 3rd, and 5th chemotherapy were similarly good (0.842, 0.858, 0.811, respectively) and those of ΔUR were similarly excellent (0.915, 0.936, 0.931, respectively).

Conclusion: In patients with bone and soft tissue sarcomas, the change of Tc-99m-MIBI image from pre-chemotherapy to early to middle of chemotherapy can predict the final histopathological tumor response to chemotherapy as accurately as the change of Tc-99m-MIBI image from pre-chemotherapy to the completion of the preoperative chemotherapy.

Key Words: bone and soft tissue sarcoma; Tc-99m-MIBI; preoperative chemotherapy; treatment monitoring; osteosarcoma; Ewing's sarcoma.

Introduction

In patients with bone and soft tissue sarcomas, the combination of aggressive chemotherapy before surgical intervention and limb-sparing surgery permits excellent quality of life and dramatic improvement of the prognosis [1]. The accurate evaluation of chemotherapeutic effects is essential for proper treatment strategy because a good response to preoperative chemotherapy is crucial to limb-sparing surgery.[2-4] In addition, early prediction of the tumor response to chemotherapy during preoperative chemotherapy would be beneficial for the planning of treatment strategy. Furthermore, noninvasive and quantitative assessment of tumor response to chemotherapy may provide prognostic information that could be useful for subsequent patient's management, because good pathological response to chemotherapy has been proved to be a predictor of good prognosis in osteosarcoma.[5-6]

Recently, there has been growing interest in using Tc-99m-hexakis-2-methoxyisobutylisonitrile (MIBI), used as a myocardial perfusion imaging agent, for tumor imaging including bone and soft-tissue tumors.[7-9] As a tumor imaging agent Tc-99m-MIBI has unique characteristics. Administration of high radionuclide activity permits radionuclide angiography, which provides information of tumor blood flow. After Tc-99m-MIBI accumulation to the tumor, the degree of washout of the tracer from the tumor reflects P-glycoprotein overexpression which implies multidrug resistance.[10,11] In addition, several studies have revealed that the change of Tc-99m-MIBI uptake from pre-chemotherapy to post-chemotherapy could reflect the chemotherapeutic effect in

patients with bone sarcomas.[8,12-14] However, there has been no report that investigated whether Tc-99m-MIBI imaging performed during preoperative chemotherapy as well as performed after the completion of the chemotherapy can equally well predict final tumor response to preoperative chemotherapy.

Therefore, the purpose of this study was to assess whether the combination of Tc-99m-MIBI scintigraphy performed before and in the early to middle of the preoperative chemotherapy can predict final histopathological tumor response to chemotherapy without deterioration of the diagnostic accuracy compared with the combination of the imaging performed before chemotherapy and after final cycle of chemotherapy in bone and soft tissue sarcomas.

MATERIALS AND METHODS

Patients

Seventy three patients (54 men and 19 women; age range, 7 to 74 years, average age, 28.8 ± 18 years) with various bone and soft-tissue sarcomas proven pathologically in specimens obtained by biopsy at pretreatment and operation after chemotherapy were recruited in this study, and all gave informed consent to participate in this study. There were 36 osteosarcomas (28 osteoblastic type, 5 chondroblastic type, 2 fibroblastic type, and 1 small cell osteosarcoma), 7 malignant fibrous histiocytomas (5 pleomorphic type, 1 spindle cell type, 1 myxoid type), 7 liposarcomas (6 myxoid liposarcoma and 1 pleomorphic liposarcoma), 6 Ewing sarcomas, 4 synovial sarcomas, 3 chondrosarcomas (2 mesenchymal chondrosarcoma and 1 extraskeletal myxoid chondrosarcoma), 3 rhabdomyosarcomas, 2 angiosarcomas, 2 leiomyosarcomas, 1 malignant schwannoma, 1 alveolar soft part sarcoma, and 1 malignant giant cell tumor. Sixty-three lesions were located in the extremities, 5 were located in pelvic area, 2 were located at shoulder, 2 were in ribs, 1 was at axilla.

Forty-six tumors were located in bone and 27 were in soft tissue.

Patients received 5 cycles of preoperative chemotherapy at intervals of 2~3 weeks. In each chemotherapy cycle, cisplatin (120 mg / m^2) was continuously infused through the intra-arterial catheter for 1 to 2 hours followed by 48 hours continuous infusion of doxorubicin (60 mg / m^2) and 72 hours infusion of caffeine.[15,16]

Study Protocol and Tc-99m-MIBI Scintigraphy

The study protocol is shown in figure 1. All patients underwent imaging with Tc-99m-MIBI at least 3 times. Before chemotherapy all patients underwent the imaging with Tc-99m-MIBI (n=73), and after 1 week of the completion of the 2 (n=20) or 3 (n=69) or 5 cycles (n=66) of chemotherapy, same radionuclide imaging procedures were performed. After the completion of the 5 cycles of chemotherapy surgical operation was performed. Then the scintigraphic predictive power for the chemotherapeutic effect was assessed in comparison with the results of the postoperative histological examination.

Radionuclide angiography was performed after bolus injection of 600 - 740 MBq (16.2 – 20 mCi) of Tc-99m-MIBI with a gamma camera equipped with a low energy high-resolution parallel-hole collimator. Data were acquired every 2 sec for 2 min. Then, planar 2-min Tc-99m-MIBI image of the lesion was obtained at 15 min after radionuclide administration with 256 x 256 matrices.

Image Analysis

In the quantitative analysis of the pre-chemotherapeutic image, a manual region of interest (ROI) was set on the lesion and an automatically generated symmetrical ROI was set on the contralateral normal area as a background. When tumor Tc-99m-MIBI uptake is weak, the ROI of the tumor was delineated carefully to cover the whole lesion by referring to the computed tomography or magnetic resonance image. In the analysis of the images obtained after 2, 3 or 5 cycles of chemotherapy,

tumor ROI was newly set to cover the whole lesion as described above. Therefore, ROI size was changed depending on the size of the tumor. When the tumor uptake of radionuclide disappeared completely the same ROI delineated at prechemotherapy was applied to calculate the indices.

Tc-99m-MIBI uptake ratio (UR) were calculated by dividing the count density of the lesion by that of the background ROI. For the prediction of the chemotherapeutic effect, the percent reduction of uptake ratio (ΔUR) was calculated as follows:

ΔUR (%) = 100[(prechemotherapy UR - postchemotherapy UR) / prechemotherapy UR]

The perfusion index (PI) was obtained by radionuclide angiography with Tc-99m-MIBI. Using the same ROI set to calculate the uptake ratio, the time-activity curve of each ROI was generated, and the PI was determined by dividing the peak count of the arterial phase of the lesion by that of the background ROI. When a peak count was not obtained, the time activity curve always showed a shoulder point, which was the flexion point between the rapid count increase due to the arterial phase and steady state or gradual count increase due to Tc-99m-MIBI accumulation to the lesion and normal tissue. Therefore, the count of the flexion point of the time activity curve was used to calculate the PI. Percent reduction of perfusion index (ΔPI) was also calculated to predict the response to chemotherapy by the following formula:

ΔPI (%) =100[(prechemotherapy PI - postchemotherapy PI) / prechemotherapy PI]

Assessment of the Chemotherapeutic effect by Histopathology

After 5 cycle of chemotherapy surgical resection of the tumor was performed. Post-operative histological assessment was performed in all patients to evaluate the response of the tumor to chemotherapy. Histological grading of the effect of chemotherapy was determined based on the degree of viable cellularity and necrosis in the largest slice of the resected tumor.[5] Grade IV (100% necrosis) and grade III (90%≤ to <100% necrosis) response were defined as good response to

chemotherapy (effective chemotherapy). Grade II (50%< to <90% necrosis) and Grade I (≤50%

necrosis) responses were defined as poor response.

Statistics

Values are expressed as the mean ± SD. Differences in PIs and URs, and ΔPIs and ΔURs between

good and poor response were analyzed by student t-test using the software JMP-5.0.1J for

Macintosh computer. To appraise the discrimination abilities of the ΔPIs and ΔURs for the

prediction of effective chemotherapy, receiver operator characteristic (ROC) curves were generated,

and the areas under the curves (A_z) were calculated. The differences between the areas under the 2

ROC curves were examined using the 1-tailed paired t test.[17,18] The optimal cutoff levels were

identified as each index value minimizing the total number of false results.[19] $P < 0.05$ was

considered statistically significant. ROC analysis was performed using the software ROCKIT 0.9B

(free software developed by Charles E. Metz, PhD for Macintosh computer).[17,18]

RESULTS

Post-operative histological examination of the resected tumors demonstrated good response in 33

patients and poor response in 40 patients. Good responders included 20 osteosarcomas, 3 malignant

fibrous histiocytomas, 2 liposarcomas, 3 Ewing sarcomas, 1 synovial sarcomas, 1

rhabdomyosarcoma, 1 leiomyosarcoma, 1 malignant schwannoma, and 1 malignant giant cell tumor.

Poor responders included 16 osteosarcomas, 4 malignant fibrous histiocytomas, 5 liposarcomas, 3

Ewing sarcomas, 3 synovial sarcomas, 3 chondrosarcomas, 2 rhabdomyosarcomas, 2 angiosarcomas,

1 leiomyosarcoma, and 1 alveolar soft part sarcoma.

All lesions showed significant tracer uptake. Accordingly, ROIs could be set without difficulty. In

2 patients after 3 cycles of chemotherapy and in 1 patient after 5 cycles of chemotherapy, PI of

Tc-99m-MIBI was not calculated because of poor bolus infusion of the radionuclide.

Before preoperative chemotherapy, there are no differences between the patients with good and poor response in PI (3.97 ± 2.51 and 3.38 ± 1.68, respectively, P=ns)) and UP (2.83 ± 0.93 and 2.74 ± 1.38, respectively, P=ns). After 2, 3, and 5 cycles of chemotherapy, in patients with good response, PI decreased to 1.81 ± 0.61 (P<0.01), 1.97 ± 1.25 (P<0.01), and 1.51 ± 0.76 (P<0.01), respectively, and UR also decreased to 1.56 ± 0.46 (P<0.01), 1.58 ± 0.51 (P<0.01), and 1.34 ± 0.46 (P<0.01), respectively. In patients with poor response, after 2, 3, and 5 cycles of chemotherapy, both PI (3.88 ± 2.17, 3.70 ± 2.77, 2.92 ± 2.48, respectively) and UR (2.64 ± 1.14, 2.61 ± 1.22, 2.19 ± 1.02, respectively) did not change significantly. Consequently, after 2, 3, and 5 cycles of chemotherapy, good responders demonstrated lower PI (P<0.05, P<0.01, P<0.01, respectively) and lower UR (P<0.05, P<0.01, P<0.01, respectively) than poor responders.

The ΔPI after 2 cycles of chemotherapy in patients with good and poor response were 36 ± 23% and -12 ± 42% (P < 0.01), respectively (Fig. 2A). The ΔPIs after 3 and 5 cycles of chemotherapy in patients with good and poor response were 45 ± 27% and -8.3 ± 50% (P < 0.0001), respectively (Fig. 2B), and 55 ± 22% and 19 ± 37% (P < 0.0001), respectively (Fig. 2C). The ΔUR obtained after 2 cycles of chemotherapy in patients with good and poor response were 34 ± 16% and -8 ± 32% (P=0.005), respectively (Fig. 3A), and those after 3 and 5 cycles of chemotherapy were 43 ± 14% and -0.7 ± 39% (P < 0.0001), respectively (Fig. 3B) and 52 ± 13% and 15 ± 27% (P < 0.0001), respectively (Fig. 3C).

The ROC curves for the predictability of effective chemotherapy of the ΔPI and ΔUR obtained after 2, 3, and 5 cycles of chemotherapy are shown in figure 4. The A_z of the ΔPI after 2, 3, and 5 cycles of chemotherapy were 0.842, 0.858, and 0.811, respectively and there were no significant differences among the values (P=0.13~0.49). The A_z of the ΔUR after 2, 3, and 5 cycles of

chemotherapy were 0.915, 0.936, and 0.931, respectively and there were no significant differences among the values (P=0.15~0.31). When A_z of the ΔPI and ΔUR in each cycles of chemotherapy is compared, A_z of the ΔPI is lower than that of ΔUR in every scintigraphic timing but only statistically significant after 5 cycles of chemotherapy (2 cycle: P= 0.16, 3 cycle: P= 0.063, 5 cycle: P= 0.0031).

The optimal thresholds obtained by ROC analysis, sensitivity, specificity, accuracy, positive and negative predictive values of each index obtained after 2, 3, and 5 cycles after chemotherapy were summarized in Table 1. The accuracy of ΔPI after 2, 3, and 5 cycles after chemotherapy was 85%, 78%, 76%, respectively, and that of ΔUR after 2, 3, and 5 cycles after chemotherapy was 85%, 89%, 85%, respectively.

On the contrary, the accuracy of PI after 2, 3, and 5 cycles after chemotherapy was 70%, 69%, 70%, respectively, and that of UR after 2, 3, and 5 cycles after chemotherapy was 70%, 69%, 72%, respectively.

Representative cases are shown in Fig 5 (good responder) and Fig 6 (poor responder).

DISCUSSION

The present study demonstrated that the combination of the Tc-99m-MIBI scintigraphies performed before chemotherapy and in the early to middle of preoperative-chemotherapy (after the 2nd and 3rd cycle) as well as after final cycle of chemotherapy (5th cycle) can accurately predict the final response to chemotherapy which was proved by histopathology after 5 cycles of chemotherapy and operation. Based on the ROC analysis, both the performance of ΔPI and ΔUR for the prediction of the chemotherapeutic effect was similarly good after 2, 3 and 5 cycle of chemotherapy. Therefore accurate prediction of the chemotherapeutic effect can be possible during

early to middle of chemotherapy. However, when ΔPI and ΔUR was compared, predictive performance of ΔUR tended to be better than that of ΔPI after 2 and 3 cycle of therapy and significantly better after the final cycle of preoperative chemotherapy.

On the contrary the diagnostic accuracies for the prediction of chemotherapeutic effect of PI and UR itself after 2, 3, and 5 cycles of chemotherapy were 69% ~ 72%, and those were inferior to that of ΔPI and ΔUR (76% ~ 89%, Table 1).

Tc-99m-MIBI has been introduced primarily as a myocardial perfusion imaging agent to replace Tl-201. Tc-99m-MIBI has lipophilic cationic properties, accumulating largely in mitochondria by its negative trans-membrane potential. Moreover, its accumulation depends on the cell viability and metabolic status in myocardial cells.[20-22] Like myocardial cells, human carcinoma cells accumulate Tc-99m-MIBI by depending on the mitochondria and plasma membrane potentials.[23,24] In addition, radionuclide angiography with sufficient dose at the administration of the tracer can permit evaluation of the tumor blood flow. Accordingly, Tc-99m-MIBI scintigraphy provide integrated information of the tumor blood flow and tracer uptake which reflect tumor viability and metabolic status.

For the evaluation of the tumor response to preoperative chemotherapy, several modalities are performed such as CT, MRI, angiography, ultrasonography, and radionuclide imaging. Conventional angiography with contrast medium can observe tumor blood flow. Although, it can offer precise morphology of tumor vasculature, quantification of the tumor blood flow is somewhat difficult compared to radionuclide angiography. CT and MRI can precisely evaluate the tumor size. However, they cannot evaluate tumor viability and metabolic status so precisely even with contrast enhancement because fibrotic change, inflammatory change, or granulation tissue secondary to tumor necrosis after chemotherapy could be enhanced. Dynamic contrast-enhanced MRI provides

information about tissue perfusion, vascular permeability, micro-vessel density [25] and may differentiate viable tumor tissue from reparative tissue. Several parameters by mathematical quantification of the dynamic data permit prediction of the chemotherapeutic response after the completion of the preoperative chemotherapy.[26] However, early prediction of chemotherapeutic effect by dynamic MRI remains to be elucidated.[27,28] The parameter calculated by dynamic MRI might mainly reflect tumor perfusion and might be similar to that obtained by radionuclide angiography with Tc-99m-labeled tracers.[28] Color Doppler ultrasound also could predict chemotherapeutic response by assessing the change of tumor blood supply and intratumoral blood flow after chemotherapy.[29] The method is relatively simple but further evaluation would be warranted including the issue of the reproducibility. Several FDG-PET studies has also demonstrated the efficacy in the prediction of the effect of chemotherapy at the end of preoperative chemotherapy,[30-34] however, sensitive FDG accumulation in chemotherapy induced inflammation or therapy related fibrous tissue has impaired the diagnostic accuracy in some cases.[31-33] Unfortunately, there has been no report in terms of the early prediction of preoperative chemotherapy using FDG PET in bone and soft tissue sarcomas.

In a previous study with 12 osteosarcoma patients, reduction of Tc-99m-MIBI uptake after completion of chemotherapy roughly correlated to the histological response.[35] Another studies with 28 bone sarcoma patients and 68 patients with bone and soft tissue sarcoma demonstrated good correlation between the reduction of Tc-99m-MIBI uptake after 3 or 4 cycles of chemotherapy and % necrosis of the tumor [36] and good predictability of tumor response to chemotherapy.[14] In the present study, in both bone and soft tissue sarcomas, reduction of tumor perfusion and Tc-99m-MIBI uptake in the early to middle of chemotherapy as well as after final cycle of chemotherapy can predict the final histological tumor response to chemotherapy. In the clinical

setting, a precise diagnostic method for the assessment of the chemotherapeutic effect at the earliest possible time after initiation of chemotherapy would be preferable. Our current study demonstrated that early imaging could permit prices estimation of chemotherapeutic effect after 2 or 3 cycle of preoperative chemotherapy as accurately as after final cycle of therapy, suggesting that the method may have an impact on modification of neoadjuvant chemotherapy protocol, on patient selection for the performance and timing of limb-sparing surgery, and on the selection of postoperative chemotherapy regimens.

MIBI has been proved to be the one of the substrates of P-glycoprotein, a product of the human multidrug resistance gene and multidrug resistance related protein.[37,38] It has been proved that Tc-99m-MIBI once accumulated in tumor cells would be washed out from the cells by P-glycoprotein and the delayed Tc-99m-MIBI uptake was related to P-glycoprotein expression, while early uptake was not.[10] Accordingly, early Tc-99m-MIBI uptake seems to reflect tumor viability more properly than delayed uptake. Therefore, as a marker of tumor viability, we analyzed only Tc-99m-MIBI uptake in early image obtained at 15 min after tracer injection.

For the assessment of tumor perfusion and Tc-99m-MIBI uptake, tumor ROI was set in each image before and after chemotherapy independently, i.e., new ROI was delineated after chemotherapy if tumor size changed to cover whole tumor more precisely instead of using the same ROI used before chemotherapy. This is because we assessed the histologic grading of chemotherapeutic effect based on the degree of cellularity and necrosis in the largest slice of the resected tumor as a gold standard of tumor response to chemotherapy. Accordingly ROI modification along with the change of the tumor size may reflect more precisely the tumor viability based on the histopathological examination.

Possible drawbacks of Tc-99m-MIBI include its high uptake by the liver and excretion to the

intestine and urinary system, which interfere with abdominal and pelvic evaluation. However, lesions of the extremities, where most bone and soft tissue sarcomas are found, are unaffected by these issues.

Since there was a great variety of tumor types included in this study, there was some dispersion in Tc-99m-MIBI tumor uptake. However, since the tumor Tc-99m-MIBI uptake reflects tumor viability and metabolic status, the degree of the change of tumor viability by chemotherapy might be reflected similarly to the change of Tc-99m-MIBI uptake among various tumor types.

CONCLUSION

The study demonstrates that the change in tumor perfusion and Tc-99m-MIBI uptake from pre-chemotherapy to early to middle of preoperative chemotherapy as well as to the final cycle of chemotherapy is highly predictive of histopathological tumor response to chemotherapy in bone and soft tissue sarcomas. This imaging technique, especially in ΔUR, might be a beneficial method in patient care and in elaborating treatment strategy during preoperative chemotherapy.

REFERENCES

1. Tsuchiya H, Tomita K, Minematsu K, et al. Limb salvage using distraction osteogenesis. A classification of the technique. *J Bone Joint Surg Br*. 1997; 79:403-411.

2. Tsuchiya H, Tomita K, Mori Y, et al. Marginal excision for osteosarcoma with caffeine assisted chemotherapy. *Clin Orthop*. 1999; 358: 27-35.

3. Jaffe N, Patel SR, Benjamin RS. Chemotherapy in osteosarcoma. Basis for application and antagonism to implementation; early controversies surrounding its implementation. *Hematol Oncol Clin North Am*. 1995; 9:825-840.

4. Eilber FR, Morton DL, Eckardt J, et al. Limb salvage for skeletal and soft tissue sarcomas. Multidisciplinary preoperative therapy. *Cancer*. 1984; 53:2579-2584.

5. Wunder JS, Paulian G, Huvos AG, et al. The histological response to chemotherapy as a predictor of the oncological outcome of operative treatment of Ewing sarcoma. *J Bone Joint Surg Am*. 1998;80:1020-1033.

6. Bielack SS, Kempf-Bielack B, Delling G, et al. Prognostic factors in high-grade osteosarcoma of the extremities or trunk: an analysis of 1,702 patients treated on neoadjuvant cooperative osteosarcoma study group protocols. *J Clin Oncol*. 2002;20:776-790.

7. Caner B, Kitapcl M, Unlu M, et al. Technetium-99m-MIBI uptake in benign and malignant bone lesions: a comparative study with technetium-99m-MDP. *J Nucl Med*. 1992; 33(3):319-324.

8. Taki J, Sumiya H, Tsuchiya H, et al. Evaluating benign and malignant bone and soft-tissue lesions with technetium-99m-MIBI scintigraphy. *J Nucl Med*. 1997; 38:501-506.

9. Buscombe JR, Cwikla JB, Thakrar DS, et al. Scintigraphic imaging of breast cancer: a review. *Nucl Med Commun*. 1997;18:698-709.

10. Taki J, Sumiya H, Asada N, et al. Assessment of P-glycoprotein in patients with malignant bone

and soft-tissue tumors using technetium-99m-MIBI scintigraphy. *J Nucl Med*. 1998; 39:1179-1184.

11. Burak Z, Ersoy O, Moretti JL, et al. The role of Tc-99m-MIBI scintigraphy in the assessment of MDR1 overexpression in patients with musculoskeletal sarcomas: comparison with therapy response. *Eur J Nucl Med*. 2001; 28:1341-1350.

12. Soderlund V, Larsson SA, Bauer HC, et al. Use of ^{99m}Tc-MIBI scintigraphy in the evaluation of the response of osteosarcoma to chemotherapy. *Eur J Nucl Med*. 1997; 24:511-515.

13. Moustafa H, Riad R, Omar W, et al. ^{99m}Tc-MIBI in the assessment of response to chemotherapy and detection of recurrences in bone and soft tissue tumours of the extremities. *Q J Nucl Med*. 2003; 47:51-57.

14. Taki J, Higuchi T, Sumiya H, et al. Prediction of final tumor response to preoperative chemotherapy by Tc-99m MIBI imaging at the middle of chemotherapy in malignant bone and soft tissue tumors: comparison with Tl-201 imaging. *J Orthop Res*. 2008, 26:411-418.

15. Tsuchiya H, Tomita K, Mori Y, et al. Marginal excision for osteosarcoma with caffeine assisted chemotherapy. *Clin Orthop*. 1999; 358: 27-35.

16. Taki J, Sumiya H, Higuchi T, et al. Prediction of myocutaneous adverse side effect due to intra-arterial chemotherapy by intra-arterial ^{99m}Tc-macroaggregated albumin administration in patients with bone and soft-tissue tumors. *J Nucl Med*. 2002; 43:1452-1456.

17. Metz CE. Some practical issues of experimental design and data analysis in radiological ROC studies. *Invest Radiol*. 1989; 24:234-245.

18. Metz CE, Herman BA, Shen JH. Maximum likelihood estimation of receiver operating characteristic (ROC) curves from continuously-distributed data. *Stat Med*. 1998; 17:1033-1053.

19. McNeil BJ, Keller E, Adelstein SJ. Primer on certain elements of medical decision making. *N Engl J Med*. 1975; 293:211-215.

20. Piwnica-Worms D, Kronauge JF, Chiu ML. Uptake and retention of hexakis (2-methoxyisobutyl isonitrile) technetium(I) in cultured chick myocardial cells. Mitochondrial and plasma membrane potential dependence. *Circulation*. 1990; 82: 1826-1838.

21. Beanlands RS, Dawood F, Wen WH, et al. Are the kinetics of technetium-99m methoxyisobutyl isonitrile affected by cell metabolism and viability? *Circulation*. 1990; 82: 1802-1814.

22. Carvalho PA, Chiu ML, Kronauge JF, et al. Subcellular distribution and analysis of technetium-99m-MIBI in isolated perfused rat hearts. *J Nucl Med*. 1992; 33: 1516-1522.

23. Delmon-Moigeon LI, Piwnica-Worms D, Van den Abbeele AD, et al. Uptake of the cation hexakis(2-methoxyisobutylisonitrile)-technetium-99m by human carcinoma cell lines in vitro. *Cancer Res*. 1990; 50: 2198-2202.

24. Maublant JC, Zhang Z, Rapp M, et al. In vitro uptake of technetium-99m-teboroxime in carcinoma cell lines and normal cells: comparison with technetium-99m-sestamibi and thallium-201. *J Nucl Med*. 1993; 34: 1949-1952.

25. Uhl M, Saueressig U, van Buiren M, et al. Osteosarcoma: preliminary results of in vivo assessment of tumor necrosis after chemotherapy with diffusion- and perfusion-weighted magnetic resonance imaging. *Invest Radiol*. 2006;41:618-623.

26. Dyke JP, Panicek DM, Healey JH, et al. Osteogenic and Ewing sarcomas: estimation of necrotic fraction during induction chemotherapy with dynamic contrast-enhanced MR imaging. *Radiology*. 2003;228:271-278.

27. Kajihara M, Sugawara Y, Sakayama K, et al. Evaluation of tumor blood flow in musculoskeletal lesions: dynamic contrast-enhanced MR imaging and its possibility when monitoring the

response to preoperative chemotherapy-work in progress. *Radiat Med*. 2007;25:94-105.

28. Ongolo-Zogo P, Thiesse P, Sau J, et al. Assessment of osteosarcoma response to neoadjuvant chemotherapy: comparative usefulness of dynamic gadolinium-enhanced spin-echo magnetic resonance imaging and technetium-99m skeletal angioscintigraphy. *Eur Radiol*. 1999;9:907-914.

29. Bramer JA, Gubler FM, Maas M, et al. Colour Doppler ultrasound predicts chemotherapy response, but not survival in paediatric osteosarcoma. *Pediatr Radiol*. 2004, 34:614-619.

30. Schulte M, Brecht-Krauss D, Werner M, et al. Evaluation of neoadjuvant therapy response of osteogenic sarcoma using FDG PET. *J Nucl Med*. 1999;40:1637-1643.

31. Iagaru A, Masamed R, Chawla SP, et al. F-18 FDG PET and PET/CT evaluation of response to chemotherapy in bone and soft tissue sarcomas. *Clin Nucl Med*. 2008;33:8-13.

32. Jones DN, McCowage GB, Sostman HD, et al. Monitoring of neoadjuvant therapy response of soft-tissue and musculoskeletal sarcoma using fluorine-18-FDG PET. *J Nucl Med*. 1996;37:1438-1444.

33. Hawkins DS, Rajendran JG, Conrad EU III, et al. Evaluation of chemotherapy response in pediatric bone sarcomas by [F-18]-fluorodeoxy-D-glucose positron emission tomography. *Cancer*. 2002;94:3277-3284.

34. Benz MR, Evilevitch V, Allen-Auerbach MS, et al. Treatment monitoring by 18F-FDG PET/CT in patients with sarcomas: interobserver variability of quantitative parameters in treatment-induced changes in histopathologically responding and nonresponding tumors. *J Nucl Med*. 2008, 49:1038-1046.

35. Soderlund V, Larsson SA, Bauer HC, et al. Use of ^{99m}Tc-MIBI scintigraphy in the evaluation of the response of osteosarcoma to chemotherapy. *Eur J Nucl Med*. 1997; 24:511-515.

36. Moustafa H, Riad R, Omar W, et al. ^{99m}Tc-MIBI in the assessment of response to chemotherapy and detection of recurrences in bone and soft tissue tumours of the extremities. *Q J Nucl Med*. 2003; 47:51-57.

37. Piwnica-Worms D, Chiu ML, Budding M, et al. Functional imaging of multidrug-resistant P-Glycoprotein with an organotechnetium complex. *Cancer Res*. 1993;53:977-984.

38. Burak Z, Moretti JL, Ersoy O, et al. ^{99m}Tc-MIBI imaging as a predictor of therapy response in osteosarcoma compared with multidrug resistance-associated protein and P-glycoprotein expression. *J Nucl Med*. 2003; 44:1394-1401.

FIGURE LEGENDS

FIGURE 1

Study protocol. Tc-99m-MIBI scintigraphy was performed before chemotherapy in all patients, and at least 2 scintigraphic studies were performed after 2, 3, or 5 cycle of chemotherapy. The change of perfusion index and uptake ratio from prechemotherapy to after each chemotherapy cycle were compared to the histopathological response to chemotherapy.

FIGURE 2

Percent reduction of perfusion index (PI) obtained from radionuclide angiography with Tc-99m-MIBI after 2 cycle (A), 3 cycle (B), and 5 cycle (C) of chemotherapy in patients with good response and poor response. Horizontal dashed line indicates threshold line derived from receiver operator characteristic curve analysis that minimized the total number of false results.

FIGURE 3

Percent reduction of Tc-99m-MIBI uptake ratio (UR) after 2 cycle (A), 3 cycle (B), and 5 cycle (C) of chemotherapy in patients with good response and poor response. Horizontal dashed line indicates threshold line derived from receiver operator characteristic curve analysis that minimized the total number of false results.

FIGURE 4

Receiver operator characteristic (ROC) curve analysis for the prediction of tumor response to chemotherapy using ΔPI and ΔUR. The areas under the ROC curve (A_z) of the percent change of

perfusion index (ΔPI) at after 2 cycle (0.842), 3 cycle (0.858), and 5 cycle (0.811) of chemotherapy were similar (A). The A_z of the percent change of Tc-99m-MIBI uptake ratio (ΔUR) at after 2 cycle (0.915), 3 cycle (0.936), and 5 cycle (0.931) of chemotherapy were also similar (B).

FIGURE 5

A 50-year-old female with pleomorphic malignant fibrous histiocytoma of the left shoulder. Before chemotherapy, radionuclide angiography with Tc-99m-MIBI demonstrated marked increase in tumor blood flow. Anterior chest image obtained 15min after the tracer injection showed intense accumulation of Tc-99m-MIBI in the left shoulder. After 2 cycles of chemotherapy, tumor blood flow and Tc-99m-MIBI uptake decreased dramatically. After 3 and 5 cycles of chemotherapy, no significant increase in tumor blood flow and Tc-99m-MIBI uptake was observed. All these findings implied a good response to chemotherapy. Wide resection of tumor was performed after 5 cycles of chemotherapy. Pathological study of the resected tumor specimen revealed no viable tumor cells.

FIGURE 6

A 16-year-old male with osteosarcoma of the right distal femur. Before chemotherapy, radionuclide angiography with Tc-99m-MIBI demonstrated marked increase in tumor blood flow and intense Tc-99m-MIBI uptake. After 2, 3, and 5 cycles of chemotherapy, tumor blood flow and tumor uptake of Tc-99m-MIBI were still increased. All these findings implied a poor response to chemotherapy. After 5 cycles of chemotherapy, resection of the tumor was performed and the pathological study of the resected tumor specimen revealed ≤ 50% tumor necrosis.
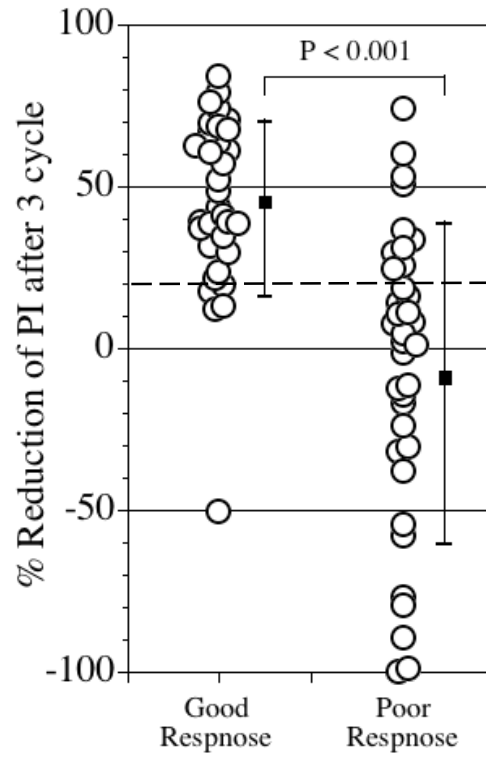
FIGURE 1

Tc-99m-MIBI imaging — 1 st chemotherapy — Tc-99m-MIBI imaging — 2 nd chemotherapy — Tc-99m-MIBI imaging — 3 rd chemotherapy — 4 th chemotherapy — Tc-99m-MIBI imaging — 5 th chemotherapy — Operation and histopathological examination
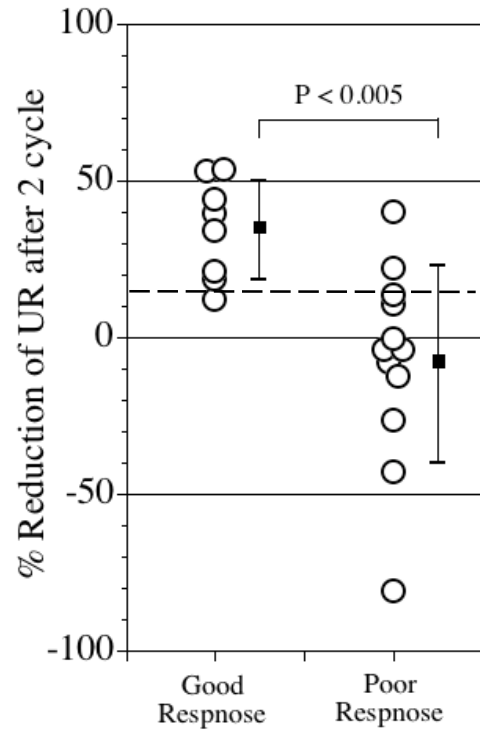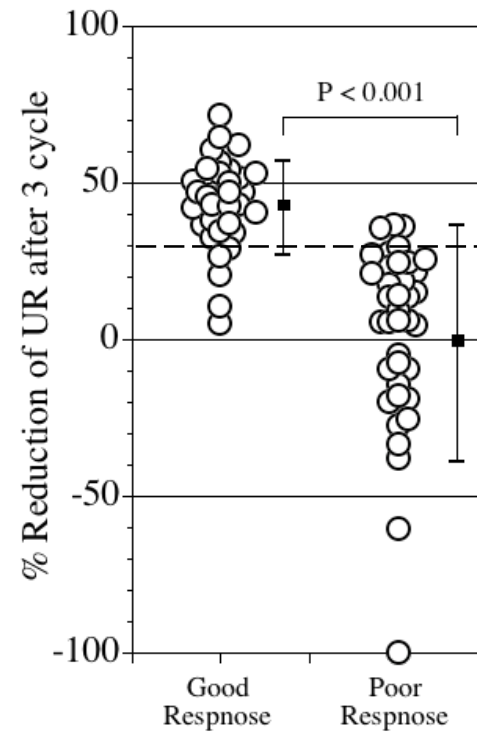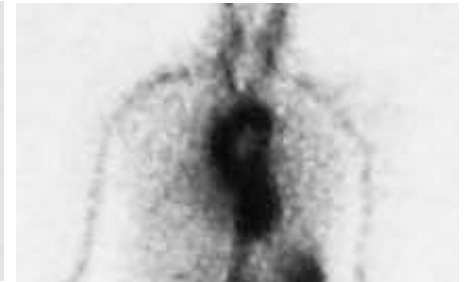
FIGURE 2

A

B

C

FIGURE 3

FIGURE 4

A

Az 2 cycle = 0.842
Az 3 cycle = 0.858
Az 5 cycle = 0.811

angio 2 cycle
angio 3 cycle
angio 5 cycle

B

Az 2 cycle = 0.915
Az 3 cycle = 0.936
Az 5 cycle = 0.931

Uptake 2cycle
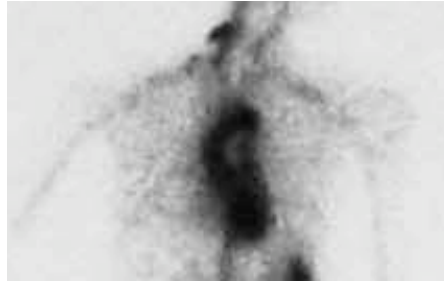Uptake 3cycle
Uptake 5cycle
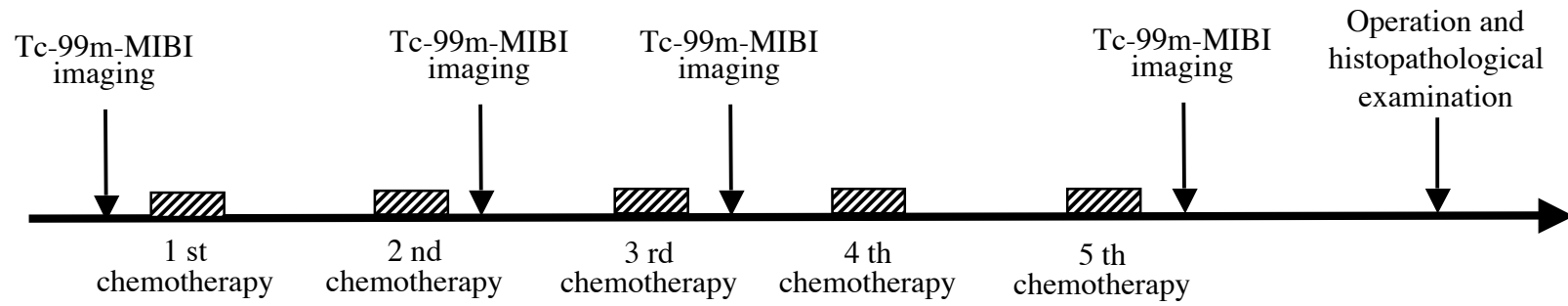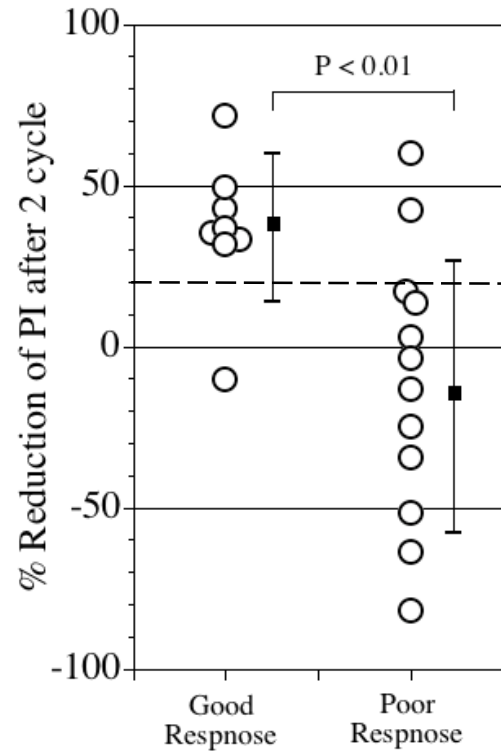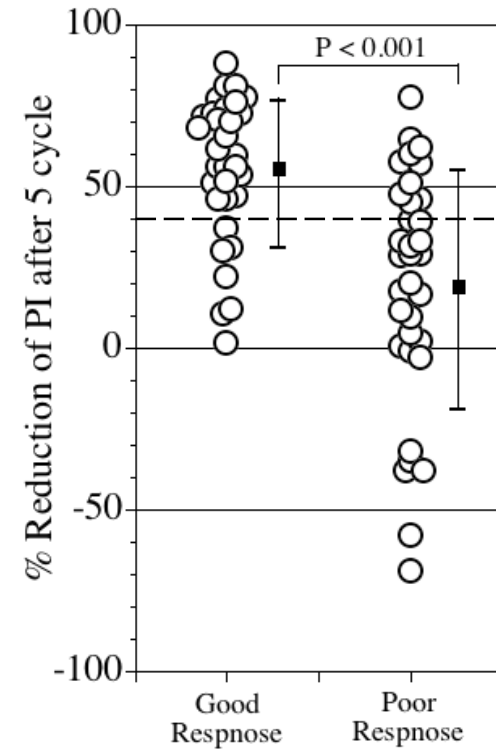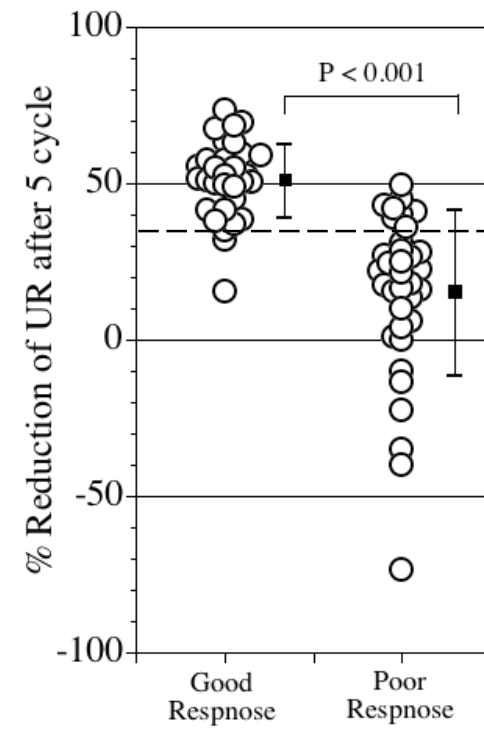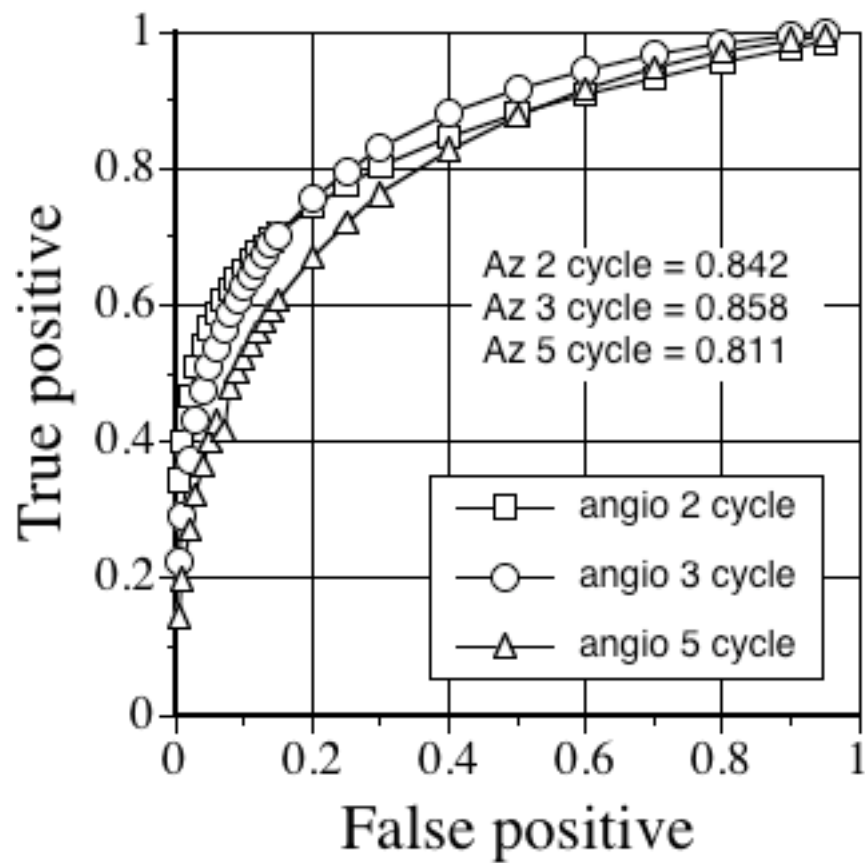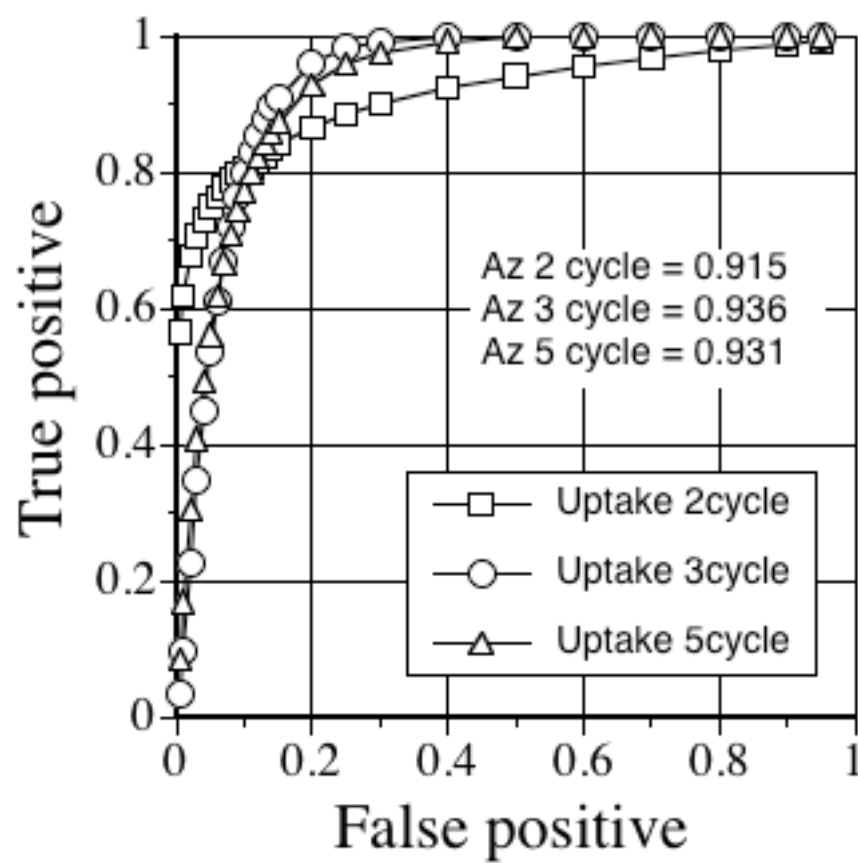
FIGURE 5

Radionuclide angiography with Tc-99m-MIBI

| Before Chemo | After 2 cycle of Chemo | After 3 cycle of Chemo | After 5 cycle of Chemo |
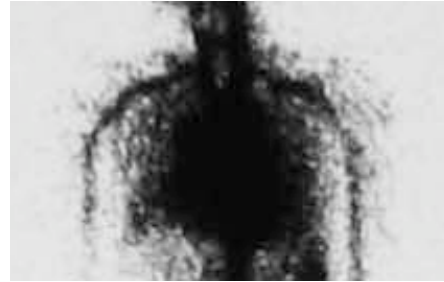
Tc-99m-MIBI 15min image

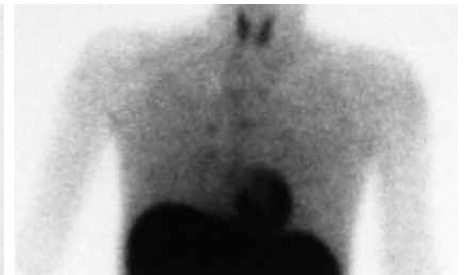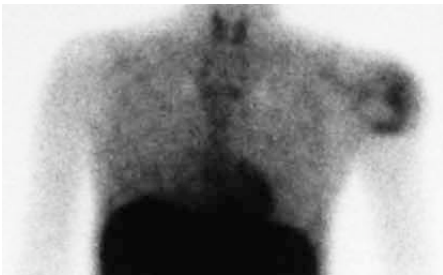| Before Chemo | After 2 cycle of Chemo | After 3 cycle of Chemo | After 5 cycle of Chemo |

FIGURE 6

Radionuclide angiography with Tc-99m-MIBI

| Before Chemo | After 2 cycle of Chemo | After 3 cycle of Chemo | After 5 cycle of Chemo |

Tc-99m-MIBI 15min image

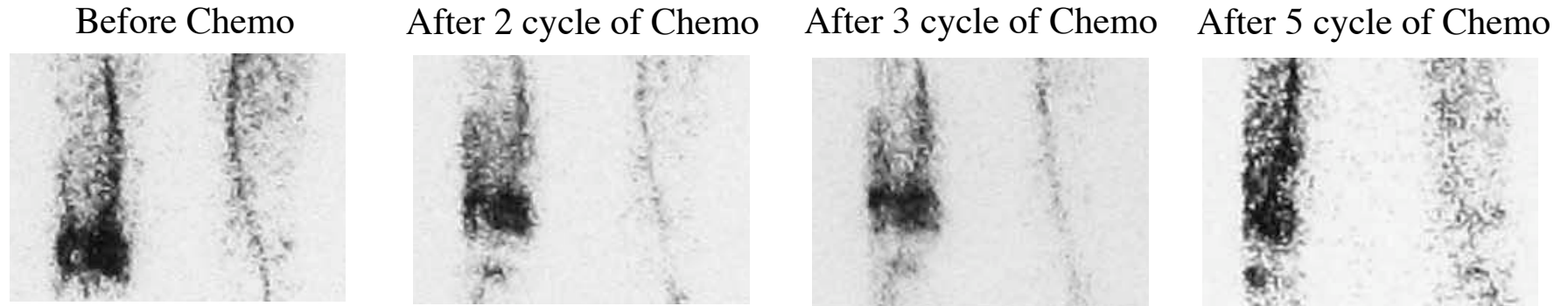| Before Chemo | After 2 cycle of Chemo | After 3 cycle of Chemo | After 5 cycle of Chemo |